Research Article

Garima Mittal and Kyong Y. Rhee*

Electrophoretic deposition of graphene on basalt fiber for composite applications

https://doi.org/10.1515/ntrev-2021-0011
received December 29, 2020; accepted March 11, 2021

Abstract: Basalt fiber (BF), because of having high strength-to-cost ratio, could be suitable for industrial applications replacing the carbon and glass fibers. However, the lack of surface functionality restricts its potential interfacial interactions with the reinforced matrix. Various surface modification approaches are used to tailor the surface properties of BFs such as coating nanomaterials and attaching chemical moieties. In this study, a successful deposition of graphene on basalt fabric was done using eco-friendly and simple electrophoretic deposition method. The confirmation of attached graphene oxide and graphene was done through the scanning electron microscope, Raman spectroscopy, and X-ray photoelectroscopy. Later, the effect of graphene coating on the thermal properties of BF was studied through thermogravimetric analysis and differential scanning calorimetry. Results show that the graphene was successfully coated on BF, and in the presence of graphene coating, the crystallization of BF delayed from 697 to 716°C because of the formation of a protective layer of graphene. Graphene-coated BF could be used further in fiber-reinforced composites to improve the interfacial interaction between the matrix and fiber.

Keywords: electrophoretic deposition, graphene, basalt fiber/fabric

1 Introduction

Fiber-reinforced composites (FRCs), because of the ease of production and durability, are being extensively used in many industries such as automobiles, aerospace, and sports. The most common examples of fibers reinforced into various matrices are carbon fibers, glass fibers, cellulose fibers, and polymer-based fibers [1,2]. Among all, glass FRCs (GFRCs) and carbon FRCs (CFRCs) are extensively studied. The commercial applications of CFRCs are limited because of their high production cost, while GFRCs are perfect for the industrial applications because of their low production cost and high strength [3,4]. Along with the expansion in GFRCs' global market, related waste is also increasing. Because of the issues during GFRCs recycling such as lower strength retention, the release of toxic gases, and high energy consumption, alternative material is required [5,6]. Recently, basalt fiber (BF) has emerged as an ideal alternative for the reinforced fiber material, owing to its high mechanical strength and exceptional environmental stability [7].

BF, also known as mineral fiber, is a natural fiber processed through the melt extrusion of solidified volcanic lava (basalt rock). Depending on the geological location of basalt rock, the chemical composition of BF varies, and therefore, their properties also vary slightly [8]. The production method of BFs is similar to the glass fiber but more environment-friendly with less energy requirement. The Young's modulus (100–110 GPa) and tensile failure (4.15–4.8 GPa) are higher than the E-type glass fiber [7–9]. In addition, BF has better resistance toward alkali solutions than glass fiber. All these properties qualify BF to be used as reinforcement in various composites for industrial applications. Despite having excellent mechanical properties, basalt FRCs (BFRCs) are not exploited up to their potential because of the surface tension during melt extrusion, which make fiber surface very smooth and the absence of reactive groups on the surface of BF [10]. Consequently, interfacial interaction between the fiber and reinforced matrix is inefficient. To upgrade the interfacial interactions, surface modification of BF is performed by treating the fiber surface using chemical or physical methods or coating nanomaterial onto the fiber surface [11–13]. Sometimes, chemical approaches use hazardous materials that increase the cost and risk and might alter the structure of fibers and

* **Corresponding author: Kyong Y. Rhee,** Department of Mechanical Engineering (BK21 four), College of Engineering, Kyung Hee University, Yongin 446-701, Republic of Korea,
e-mail: rheeky@khu.ac.kr
Garima Mittal: Department of Mechanical Engineering (BK21 four), College of Engineering, Kyung Hee University, Yongin 446-701, Republic of Korea

their performance [12,13]. In contrast, coating nanomaterials on the fiber surface introduces the additional property to the fiber [14–18]. In addition, coating nanomaterials on fibers introduce a hierarchical feature, helping in forming a continuous nexus throughout the reinforced matrix [15]. Many coating methods are reported in the literature such as dip coating, spray coating, chemical vapor deposition (CVD), and electrophoretic deposition (EPD) [19,20]. Despite being cost-efficient and straightforward approaches, dip coating and spray coating lack the efficiency because of the unevenly deposited and poorly adhered coating [21]. CVD is used to deposit carbon-based nanomaterials on different fibers [22–24]. However, the extreme conditions of CVD (high temperature) are not suitable for BFs (operating temperature limit ~650°C) as it compromises their strength [23,25].

EPD is a widely practiced industrial method that is simple, fast, environmentally safe, and cost-efficient. Electrophoretically deposited coatings are homogenous, compact, and well adhered to the substrate [26]. In a typical EPD process, charged particles suspended into a dispersed medium migrate toward the counter-charged electrodes dipped into the stable suspension in the presence of an applied electric field. A consequent stacking of the material forms a homogenous coating. The coating properties can be regulated by modifying the mass and concentration of the suspended material, applied potential, and deposition time [26]. EPD does not require expensive apparatus or hazardous chemicals and usually used at room temperature and non-vacuum conditions. Moreover, the process does not affect the basic properties of the BF adversely. EPD allows coating a wide range of conductive materials on complex surfaces. The other benefit of using EPD is that the nanomaterial can be coated directly onto the fiber surface (no sizing agent or chemical required). Therefore, in this study, we are using EPD to deposit the nanomaterial on BF's surface. Among nanomaterials, graphene is an excellent choice for reinforcing various matrices because of its extraordinary mechanical, thermal, and electrical properties and good chemical stability [27,28]. In addition, the layered structure of graphene allows it to be flattened and parallel to the fiber surface in the presence of shearing force [29]. To the best of our knowledge, not many reports available on the direct coating of graphene on BF. Most of the available reports are based on graphene attachment to the BF surface through chemical groups or coupling agents [30–33].

Our objective is to coat graphene flakes directly on the surface of BF using EPD (without any chemical agent), which could improve the interfacial interactions of BF with the reinforced matrix. This is a preliminary study where we are focusing on the successful deposition of graphene on the fiber. Although there are plenty of reports available on EPD of graphene on carbon fibers as a substrate, to the best of our knowledge there is no report on the deposition of graphene on BF using EPD. For that, at first graphene oxide (GO) layer was deposited using EPD and later thermochemically reduced into graphene. The deposition of graphene was confirmed using Field Emission Scanning Electron Microscopes (FE-SEM), X-ray photoelectric spectroscopy (XPS), and Raman spectroscopy. Later, the effect of coated material on the thermal performance of BF was also examined through thermogravimetric analysis (TGA) and differential scanning calorimetry (DSC). Our future work would be focused on the optimization of the deposition parameters such as voltage and time for EPD of graphene on BF.

2 Experimental

2.1 Materials

A plain-woven type of basalt fabric was obtained from Seotech, Korea. Graphite, potassium permanganate, and reagent grade hydrazine hydrate were obtained from Sigma Aldrich, Korea. Sulfuric acid, hydrochloric acid, and hydrogen peroxide were obtained from Daejung Chemicals, Korea.

2.2 Synthesis of GO

GO was prepared using the modified Hummer's method [34]. Briefly, 3 g of graphite was mixed with 70 mL of H_2SO_4 followed by slow mixing of 9 g $KMnO_4$ in the presence of an ice-bath. The solution was continuously stirred at 35°C for 30 min, followed by slow mixing of 150 mL water into the solution. While maintaining the temperature at 95°C, the solution was stirred for 15 min, followed by mixing 500 mL water. After mixing for 5 min, as the temperature of the solution reduces, 15 mL hydrogen peroxide (30%) was mixed dropwise, which changed the solution color from brown to bright yellow with the visible presence of bubbles. Later, the resulting mixture was kept undisturbed to collect the precipitated material, which was further washed with 1% HCl solution. After repeated washing and drying with water, GO powder was obtained.

2.3 EPD of graphene on BF

To deposit the graphene on BF, at first GO was deposited on through EPD because a homogenous aqueous suspension of the coating material is a prerequisite for EPD set-up, which is quite difficult for graphene because of its agglomeration formation tendency. GO forms a highly stable colloidal suspension in water because of the presence of various oxygen-containing groups such as epoxide, hydroxyl, and carbonyl groups attributing to its strong hydrophilicity. As EPD set-up requires a conductive material as a substrate, and BF is a non-conductive material made up of melted lava rocks, we placed the basalt fabric on a copper sheet acting as an electrode. Our EPD set-up contained 2 L of bath solution of GO with 2 mg/mL concentration in a 2-L beaker, which was continuously stirred using magnetic stirrer during deposition. Copper plates (99.96% purity) with the dimensions of 10 × 15 × 0.2 mm were used as +ve and −ve electrodes. The targeted BF was attached through a cellophane tape to the anode as the EPD of GO is an anodic deposition because of the negative charge on the GO sheet. The distance between both the electrodes was ~2 cm. During the experiment, using a DC bench power bench supply (RS Pro IPS-303DD, China), a voltage of 5 V was applied for 5 min. After deposition, the coated BF was washed by dipping twice in DI water to remove loosely attached GO (just by dipping into the GO solution). Later, the GO-coated BF was dried for 12 h at 50°C temperature. The resulting BF was termed as GO-BF.

Further, the reduction of GO-BF was performed through thermochemical reduction. GO-BF was kept for 24 h at 100°C in a glass Petri-plate containing a tissue dipped in hydrazine hydrate (~2–3 mL). Being a strong reducing agent, hydrazine hydrate reduced the GO sheets grafted on BF, and the resulting fabric material was termed as rGO-BF.

The schematic representation of the deposition of graphene on basalt fabric through the EPD process is depicted in Figure 1.

2.4 Characterization

The morphological changes on the surface of basalt fabric after graphene deposition were analyzed using FE-SEM (LEO SUPRA 55, GENESIS, 2000). To improve the quality

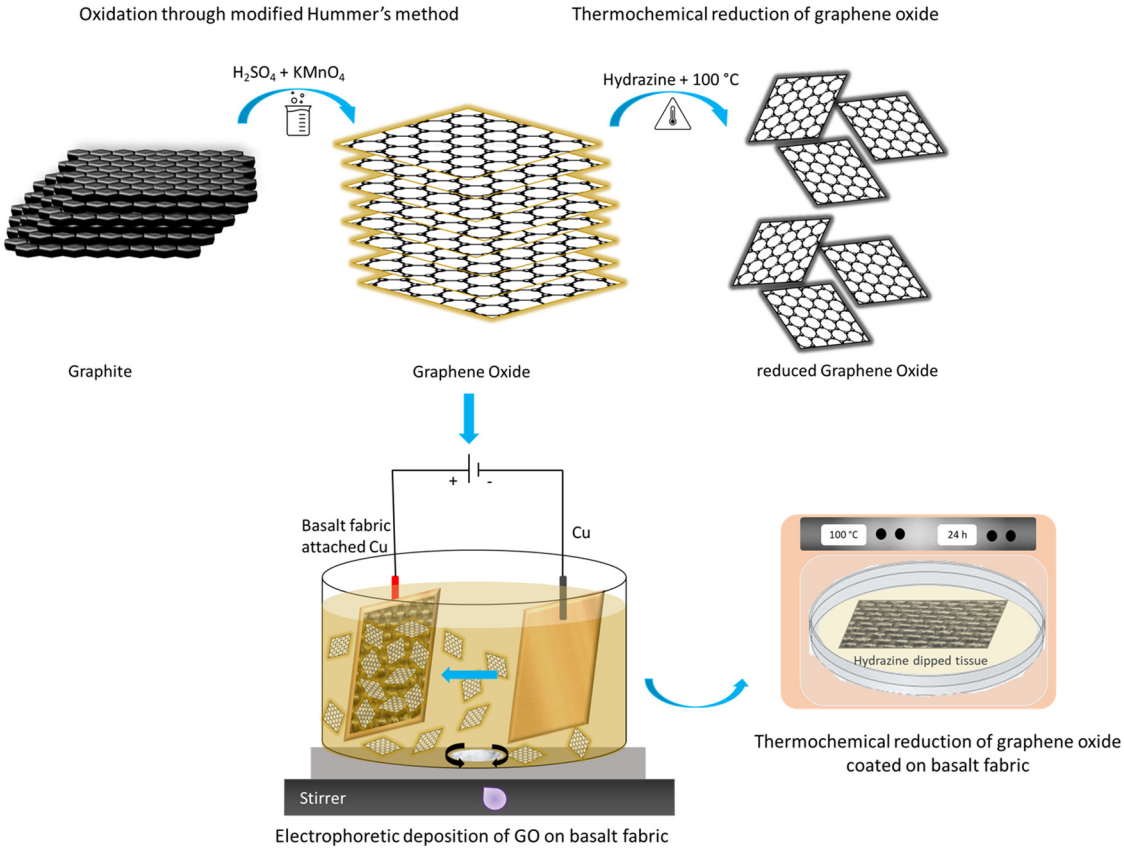

Figure 1: Schematic representation of deposition of graphene on basalt fabric through the EPD process.

of obtained images, platinum was sputtered on samples. To confirm the presence of graphene and GO on BF Raman spectroscopy (RFS 100/S (Bruker, λ = 532 nm)) was performed from 100 to 3,200 cm^{-1} wavelengths. Further confirmation was done using XPS (K-Alpha (Thermo Electron), Thermo Fischer Scientific). The effect of graphene coating on the thermal properties of BF was analyzed through TGA (SQT 600 model), which was done from room temperature to 800°C with a temperature ramp rate of 10°C/min in the presence of nitrogen gas (100 mL/min).

3 Results and discussion

Morphological properties of bare BF, GO-BF, and rGO-BF were compared using FE-SEM. Figure 2(a–c) shows the FE-SEM images of BF, GO-BF, and rGO-BF, respectively. As can be seen, BF's surface was smoother before EPD of GO, and only some residues of the sizing agent were present. On the contrary, after EPD, the surface of GO-BF and rGO-BF became comparatively rougher, and wrinkled GO and graphene flakes could be observed [35]. During EPD, because of applied electric field, negatively charged GO flakes start migrating toward the BF attached to the positive electrode and deposit on it. Later, GO flakes coated on the BF surface were thermochemically reduced into rGO flakes. The multi-layered stacking of GO oxide sheets reduced into few-layered transparent graphene after reduction. The longer flakes of graphene attached to the surface of BF in rGO-BF could be seen in Figure 2(c). These free end graphene flakes could play a crucial role in establishing interfacial connections with the adjacent BF and form a continuous electrically and thermally conductive connection throughout the fabric.

The confirmation of coated GO and graphene was done using Raman spectroscopy, a very fast, non-destructive tool to analyze the crystallinity of carbon materials. Figure 3 compares the Raman graphs of bare BF, GO-BF, and rGO-BF. Two broad peaks ascribed to the basaltic glass were observed at 490 and 970 cm^{-1} in bare BF. After coating, these peaks were dominated by characteristic graphitic bands in GO-BF and rGO-BF samples. The band that appears at around 1,350 cm^{-1} is because of the defects that occurred in the graphitic ring and known as D-band. The

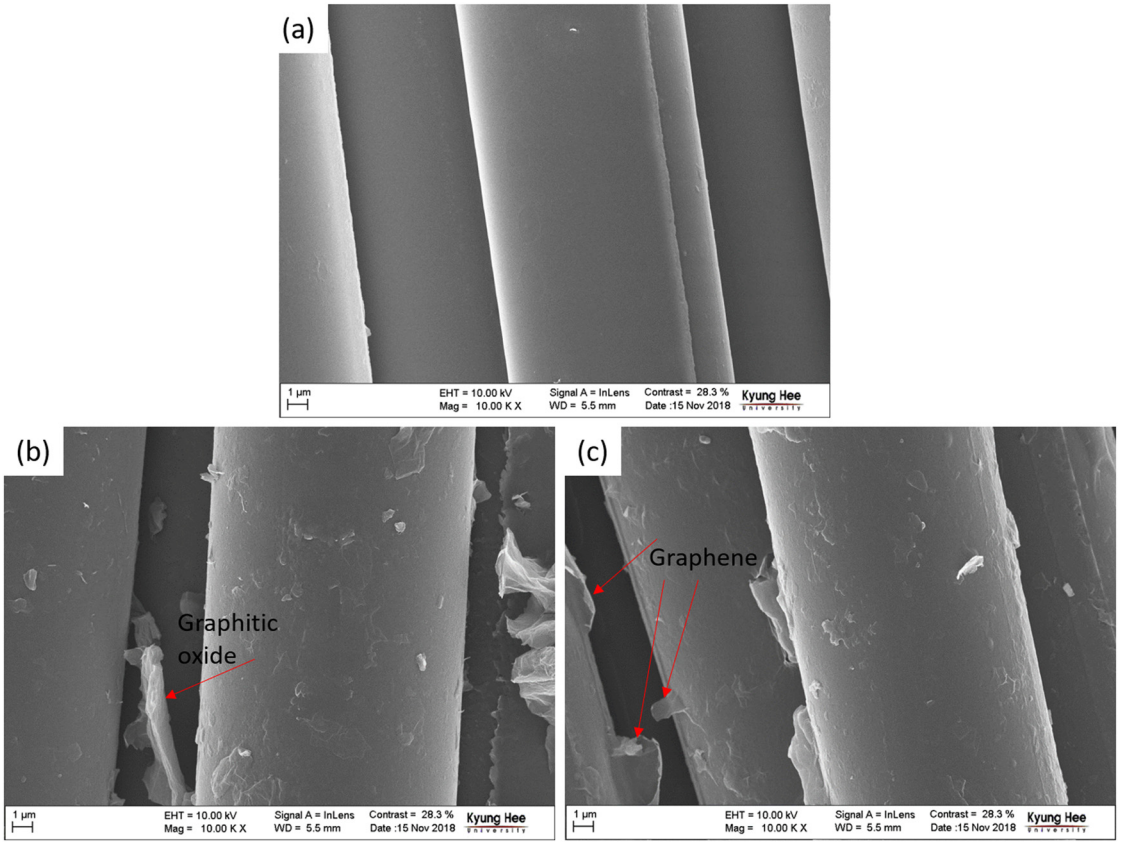

Figure 2: FE-SEM images of: (a) bare BF; (b) GO-coated BF (GO-BF); (c) graphene-coated BF (rGO-BF).

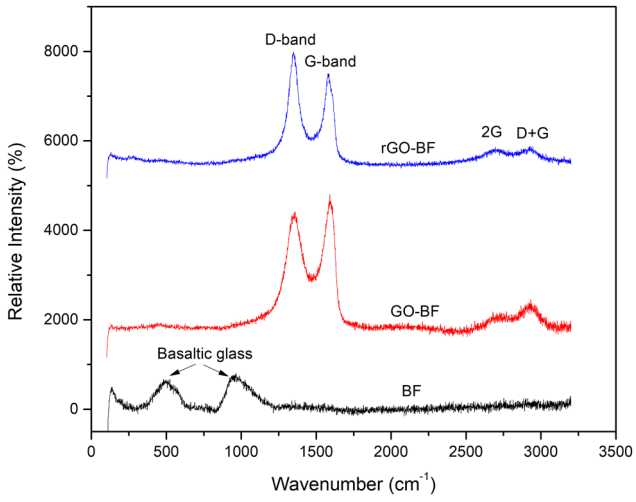

Figure 3: Raman spectra of bare BF, GO-coated BF (BF-GO), and graphene-coated BF (BF-rGO).

band that appears at 1,580 cm^{-1} indicates the crystallinity of the graphitic ring in the carbon material. As can be compared, in rGO-BF's spectrum, the D-band is more intense, indicating the introduced defects during the thermo-chemical reduction of GO coated on BF. After removing the vast number of oxygen-containing groups, the ring-opening of epoxides occurs, and the number of unrepaired defects increases. The confirmation of chemical and structural changes during reduction was done by the intensity ratio of defects and graphitic rings (I_D/I_G). A higher I_D/I_G value represents the increased number of defects. The I_D/I_G of GO-BF (0.88) was lower than that of rGO-BF (1.24), which was in accord with the many literatures based on the chemical reduction of graphene and confirmed the formation of rGO [36].

The successful reduction of GO into Gr on BF was confirmed through XPS, and the data are shown in Figure 4. Figure 4(a) represents the survey spectrum of

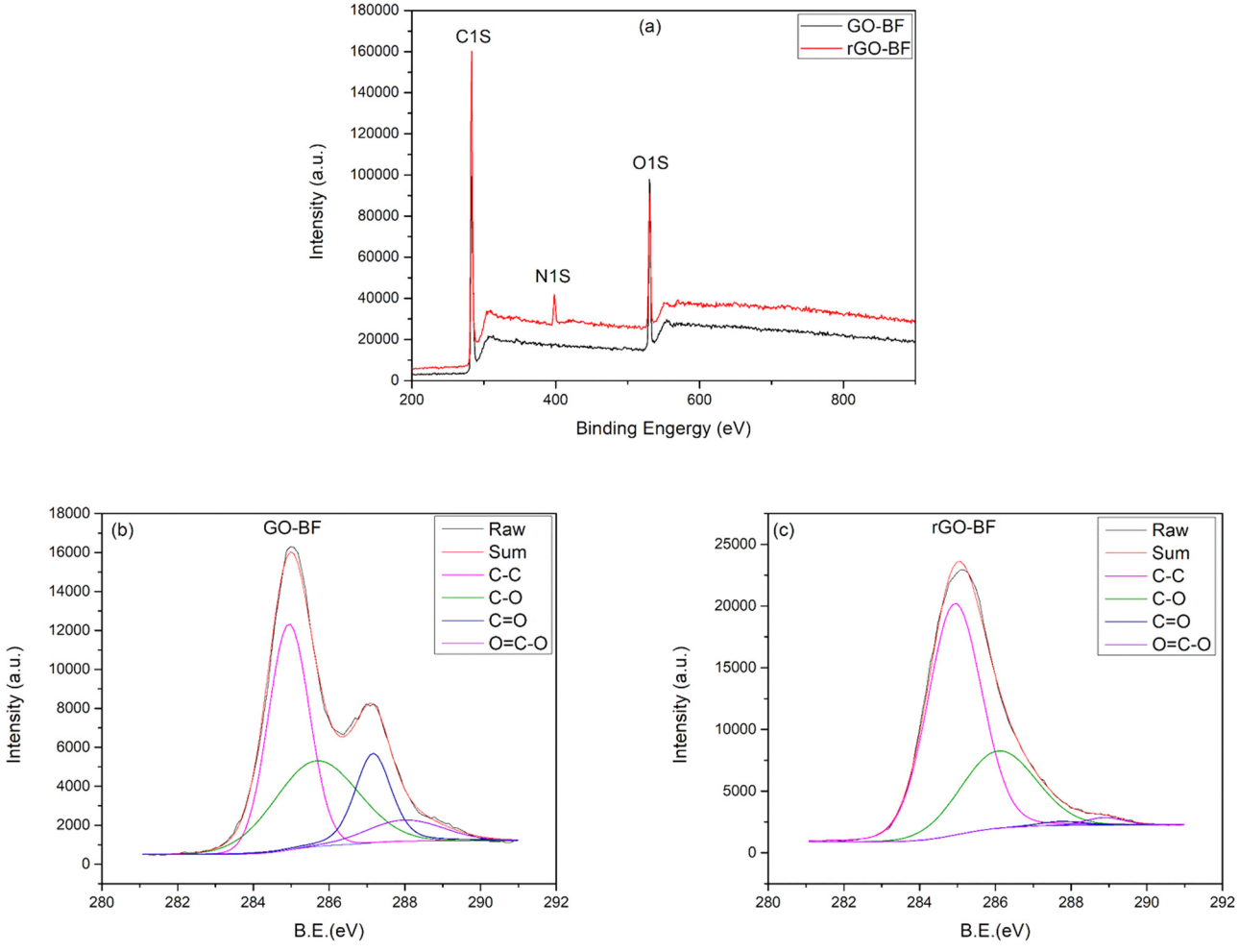

Figure 4: (a) XPS survey spectra of GO-coated BF (GO-BF) and reduced GO-coated BF (rGO-BF); (b) and (c) represent the C 1s spectra of GO-BF and rGO-BF, respectively.

Table 1: Atomic weight percentages of C 1s and O 1s spectra of the GO-coated BF and graphene-coated BF obtained through XPS

Sample	C (at.%)	O (at.%)	C/O
GO-BF	77.03	22.97	3.35
rGO-BF	83.63	16.37	5.11

GO (black) and graphene (red) coated BF. Typical C 1s and O 1s peaks could be seen at around 284 and 532 eV, respectively, in both the cases, along with a trace of N 1s peak around 400 eV in graphene-coated BF. This nitrogen peak could be attributed to the strong reducing agent hydrazine used to reduce GO [37]. Typical C 1s-related peaks are shown in Figure 4(b) and (c) for both GO-BF and rGO-BF. When graphite is oxidized through modified Hummer's method, oxygen-containing functional groups (such as hydroxyl, epoxide, carbonyl, and carboxyl) attach to the GO surface responsible for the hydrophilic nature of the material. For both GO-BF and rGO-BF, the C 1s was deconvoluted into three peaks, *i.e.*, C–C at 284.6 eV, C–O (epoxy and hydroxyl) at ~286.5 eV and C═O (carboxyl) at ~288.8 eV [38]. As a result of the reduction process, these oxygen-containing peaks significantly diminish, and C–C peak intensifies, suggesting the successful removal of oxygenated functional groups in graphene sheets. With the decomposition of oxygenated groups, a considerable deformation of the GO structure occurs, justifying the exfoliation during the process [39]. This is in accord with the Raman analysis, where D-band becomes intense after thermochemical reduction. Besides, the elemental analysis of obtained XPS data revealed the same outcomes. As shown in Table 1, the C/O ratio for GO-BF sample increased after thermochemical reduction, proving the presence of more oxygen-containing functional groups in GO-BF and *vice versa* rGO-BF [40].

The effects of the GO and graphene coatings on the thermal properties of BF were analyzed through DSC (a) and TGA (b) in Figure 5. Following a similar trend, all the samples show the glass transition temperature around 153°C. According to the published reports [41], when BF is heated, the crystalline structure of the minerals present on the fiber surface changes. With the applied temperature, migration of the divalent cations (Ca^{2+}, Mg^{2+}, and Fe^{2+}) to the periphery of the fiber from its core takes place [41]. After migration, these divalent cations take part in redox reactions by acting as nuclei in the crystallization process. Diverse crystalline phases emerge at different temperatures consequently, affecting the crystalline mechanism of the fiber and making it brittle. It seems because of the coating, bare BF shows lower crystalline peak temperature, *i.e.*, at 697°C. While GO and graphene coatings acting as a protective layer delay the crystallization, the crystallization peak temperatures were 708 and 716°C for GO-BF and rGO-BF, respectively. Various studies report the similar behavior of a coating on BF. For instance, Gutnikov *et al.* [42] published a study where crystallization was slowed down by a nanolayer coating of alkaline oxide formed during the heating.

Figure 5(b) shows the TGA curves of BF, GO-BF, and rGO-BF. It can be seen from the curves that BF shows excellent thermal stability and does not show a weight loss (no burning). The properties and constituents (such as minerals, silicates, alumina, Fe_2O_3, FeO, MgO, CaO, Na_2O, K_2O, and TiO_2) of BF vary with the origin of the lava rock. BF and GO-BF show a similar weight gain pattern, and the total weight gain was 3.3 and 1.9%, respectively. While in the case of rGO-BF, the total weight loss was almost zero. When BF is heated, divalent cations

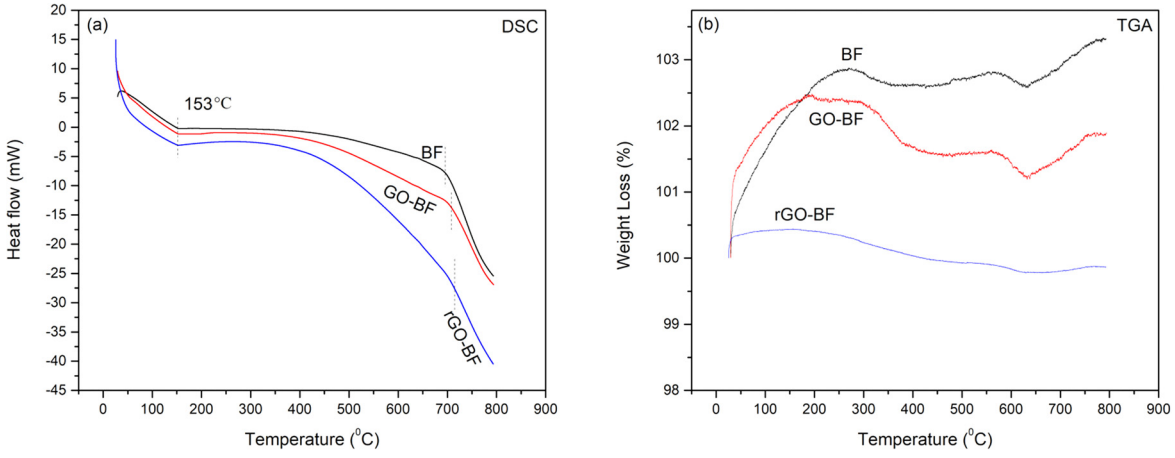

Figure 5: DSC-heating curve (a) and TGA (b) curves of bare BF, GO-coated BF (GO-BF), and graphene-coated BF (rGO-BF).

move to the surface of the fiber from the center, participating in redox reactions. A reaction might have possibly occurred between these surface particles and the environment, leading to the weight gain of the fiber [43]. In the case of GO-BF, further two significant weight losses can be observed. First weight loss (between 100 and 300°C) could be ascribed to the degradation of oxygen-containing functional groups present on the GO surface and the second one (after 350°C) could be attributed to the decomposition of more stable oxygen groups into CO_2 and CO [40]. For rGO-BF, graphene acts as a protective layer and probably restricts the interaction between the environment and the BF surface. Because of the small number of oxygen-containing functional groups, graphene does not go under degradation like GO. Therefore, it could be concluded that the deposition of graphene on BF improves its thermal stability.

4 Conclusion

BF could be a perfect candidate considering the worldwide inclination toward green technologies. It could replace the glass and BFs in FRCs with low production cost and excellent environmental stability. However, the smooth surface and lack of surface functional groups restrict the full potential use of BFRCs. Therefore, to modify the basalt surface properties, graphene was coated through EPD, where GO was deposited on basalt fabric followed by its thermochemical reduction into graphene. The confirmation of successful attachment of graphene flakes was done using FE-SEM, Raman, and XPS. The effects of graphene coating on the thermal stability of BF were studied through TGA and DSC that confirmed that the graphene coating act as a protective coating during crystallization of BF at a higher temperature. The crystalline peak temperature was shifted from 697°C for base BF to 716°C for rGO-BF. This is a preliminary study with a goal of successful deposition of graphene on BF using EPD. Our further research would focus on the optimization of the deposition parameters, such as voltage and time. Later, the effect of graphene-coated BF on the performance of reinforced matrix assuming graphene-coated BF might significantly improve the interfacial interactions between reinforced polymer/cement/metal matrix and fiber.

Funding information: This work was supported by the Basic Science Research Program through the National Research Foundation of Korea (NRF) funded by the Ministry of Education, Science and Technology (project number: 2020R1A2B5B02002203).

Author contributions: All the authors have accepted responsibility for the entire content of this manuscript and approved its submission.

Conflict of interest: The authors state no conflict of interest.

References

[1] Prashanth S, Subbaya KM, Nithin K, Sachhidananda S. Fiber reinforced composites – a review. J Mater Sci Eng. 2017;6:2–6.
[2] Syafiq RM, Sapuan SM, Zuhri MR. Effect of cinnamon essential oil on morphological, flammability and thermal properties of nanocellulose fibre – reinforced starch biopolymer composites. Nanotechnol Rev. 2020;9(1):1147–59.
[3] Amiri A, Krosbakken T, Schoen W, Theisen D, Ulven CA. Design and manufacturing of a hybrid flax/carbon fiber composite bicycle frame. Proc Inst Mech Eng Part P J Sports Eng Technol. 2017;232(1):28–38.
[4] Sathishkumar TP, Satheeshkumar S, Naveen J. Glass fiber-reinforced polymer composites – a review. J Reinf Plast Compos. 2014;33(13):1258–75.
[5] Zabihi O, Ahmadi M, Liu C, Mahmoodi R, Li Q, Ghandehari Ferdowsi MR, et al. A sustainable approach to the low-cost recycling of waste glass fibres composites towards circular economy. Sustainability. 2020;12:2.
[6] Karuppannan Gopalraj S, Kärki T. A review on the recycling of waste carbon fibre/glass fibre-reinforced composites: fibre recovery, properties and life-cycle analysis. SN Appl Sci. 2020;2(3):433.
[7] Fiore V, Scalici T, Di Bella G, Valenza A. A review on basalt fibre and its composites. Compos Part B Eng. 2015;74:74–94.
[8] Dhand V, Mittal G, Rhee KY, Park S-J, Hui D. A short review on basalt fiber reinforced polymer composites. Compos Part B Eng. 2015;73:166–80.
[9] Deák T, Czigány T. Chemical composition and mechanical properties of basalt and glass fibers: a comparison. Text Res J. 2009;79(7):645–51.
[10] Wei B, Song S, Cao H. Strengthening of basalt fibers with nano-SiO2–epoxy composite coating. Mater Des. 2011;32(8):4180–6.
[11] Mittal G, Rhee KY, Mišković-Stanković V, Hui D. Reinforcements in multi-scale polymer composites: processing, properties, and applications. Compos Part B Eng. 2018;138:122–39.
[12] Jain N, Singh VK, Chauhan S. Review on effect of chemical, thermal, additive treatment on mechanical properties of basalt fiber and their composites. J Mech Behav Mater. 2017;26(5–6):205–11.
[13] Overkamp T, Mahltig B, Kyosev Y. Strength of basalt fibers influenced by thermal and chemical treatments. J Ind Text. 2016;47(5):815–33.

[14] Ling Y, Zhang P, Wang J, Taylor P, Hu S. Effects of nanoparticles on engineering performance of cementitious composites reinforced with PVA fibers. Nanotechnol Rev. 2020;9(1):504–14.
[15] Kim M, Lee T-W, Park S-M, Jeong YG. Structures, electrical and mechanical properties of epoxy composites reinforced with MWCNT-coated basalt fibers. Compos Part A Appl Sci Manuf. 2019;123:123–31.
[16] Wang X, Feng J, Feng J, Tian Y, Luo C, Sun M. Basalt fibers coated with nano-calcium carbonate for in-tube solid-phase microextraction and online analysis of estrogens coupled with high-performance liquid chromatography. Anal Methods. 2018;10(19):2234–41.
[17] Zhang H, Li X, Qian W, Zhu J, Chen B, Yang J, et al. Characterization of mechanical properties of epoxy/nano-hybrid composites by nanoindentation. Nanotechnol Rev. 2020;9(1):28–40.
[18] Guo Z, Huang C, Chen Y. Experimental study on photocatalytic degradation efficiency of mixed crystal nano-TiO2 concrete. Nanotechnol Rev. 2020;9(1):219–29.
[19] Karger-Kocsis J, Mahmood H, Pegoretti A. Recent advances in fiber/matrix interphase engineering for polymer composites. Prog Mater Sci. 2015;73:1–43.
[20] Zakaria MR, Akil HM, Omar MF, Abdullah MMAB, Rahman AAA, Othman MBH. Improving flexural and dielectric properties of carbon fiber epoxy composite laminates reinforced with carbon nanotubes interlayer using electrospray deposition. Nanotechnol Rev. 2020;9(1):1170–82.
[21] Zhang J, Zhuang R, Liu J, Mäder E, Heinrich G, Gao S. Functional interphases with multi-walled carbon nanotubes in glass fibre/epoxy composites. Carbon. 2010;48(8):2273–81.
[22] Mittal G, Rhee KY. Chemical vapor deposition-based grafting of CNTs onto basalt fabric and their reinforcement in epoxy-based composites. Compos Sci Technol. 2018;165:84–94.
[23] Mittal G, Rhee KY. Hierarchical structures of CNT@basalt fabric for tribological and electrical applications: Impact of growth temperature and time during synthesis. Compos Part A Appl Sci Manuf. 2018;115:8–21.
[24] De Greef N, Zhang L, Magrez A, Forró L, Locquet J-P, Verpoest I, et al. Direct growth of carbon nanotubes on carbon fibers: effect of the CVD parameters on the degradation of mechanical properties of carbon fibers. Diam Relat Mater. 2015;51:39–48.
[25] Singha K. A short review on basalt fiber. Int J Text Sci. 2012;1:19–28.
[26] Besra L, Liu M. A review on fundamentals and applications of electrophoretic deposition (EPD). Prog Mater Sci. 2007;52(1):1–61.
[27] Mittal G, Dhand V, Rhee KY, Park S-J, Lee WR. A review on carbon nanotubes and graphene as fillers in reinforced polymer nanocomposites. J Ind Eng Chem. 2015;21:11–25.
[28] Yan Y, Nashath FZ, Chen S, Manickam S, Lim SS, Zhao H, et al. Synthesis of graphene: potential carbon precursors and approaches. Nanotechnol Rev. 2020;9(1):1284–314.
[29] Kim J, Cote LJ, Huang J. Two dimensional soft material: new faces of graphene oxide. Acc Chem Res. 2012;45(8):1356–64.
[30] Tkachev S, Kraevskii S, Kornilov D, Voronov V, Gubin S. Graphene oxide on the surface of basalt fiber. Inorg Mater. 2016;52:1254–8.
[31] Zhou S, Wang J, Wang S, Ma X, Huang J, Zhao G, et al. Facile preparation of multiscale graphene-basalt fiber reinforcements and their enhanced mechanical and tribological properties for polyamide 6 composites. Mater Chem Phys. 2018;217:315–22.
[32] Wang J, Zhou S, Huang J, Zhao G, Liu Y. Interfacial modification of basalt fiber filling composites with graphene oxide and polydopamine for enhanced mechanical and tribological properties. RSC Adv. 2018;8(22):12222–31.
[33] He H, Yang P, Duan Z, Wang Z, Liu Y. Reinforcing effect of hybrid nano-coating on mechanical properties of basalt fiber/poly(lactic acid) environmental composites. Compos Sci Technol. 2020;199:108372.
[34] Chen J, Yao B, Li C, Shi G. An improved Hummers method for eco-friendly synthesis of graphene oxide. Carbon. 2013;64:225–9.
[35] Wu Y, Tang B, Liu K, Zeng X, Lu J, Zhang T, et al. Enhanced flexural properties of aramid fiber/epoxy composites by graphene oxide. Nanotechnol Rev. 2019;8(1):484–92.
[36] Tlhomelang K, Jahed N, Baker P, Iwuoha E. Metallo-graphene nanocomposite electrocatalytic platform for the determination of toxic metal ions. Sens (Basel, Switz). 2011;11:3970–87.
[37] Chua CK, Pumera M. The reduction of graphene oxide with hydrazine: elucidating its reductive capability based on a reaction-model approach. Chem Commun. 2016;52(1):72–5.
[38] Carolina A, Moraes M, de Araujo Lima B, Fonseca de Faria A, Brocchi M, Alves O. Graphene oxide-silver nanocomposite as a promising biocidal agent against methicillin-resistant Staphylococcus aureus. Int J Nanomed. 2015;10:6847–61.
[39] Gurzęda B, Buchwald T, Nocuń M, Bąkowicz A, Krawczyk P. Graphene material preparation through thermal treatment of graphite oxide electrochemically synthesized in aqueous sulfuric acid. RSC Adv. 2017;7(32):19904–11.
[40] Soltani T, Kyu, Lee B. A benign ultrasonic route to reduced graphene oxide from pristine graphite. J Colloid Interface Sci. 2017;486:337–43.
[41] Chen X, Zhang Y, Hui D, Chen M, Wu Z. Study of melting properties of basalt based on their mineral components. Compos Part B Eng. 2017;116:53–60.
[42] Gutnikov SI, Manylov MS, Lipatov YV, Lazoryak BI, Pokholok KV. Effect of the reduction treatment on the basalt continuous fiber crystallization properties. J Non-Cryst Solids. 2013;368:45–50.
[43] Huang Y, Lu H, Gu H, Fu J, Mo S, Wei C, et al. A CNT@MoSe2 hybrid catalyst for efficient and stable hydrogen evolution. Nanoscale. 2015;7(44):18595–602.